Highly Ordered Assembly of Single-Domain Dichloropentacene over Large Areas on Vicinal Gold Surfaces

Jun Wang,[†,*] Irvinder Kaur,[‡] Bogdan Diaconescu,[†,§] Jian-Ming Tang,[†] Glen P. Miller,[‡] and Karsten Pohl[†]

[†]Department of Physics and Materials Science Program and [‡]Department of Chemistry and Materials Science Program, University of New Hampshire, Durham, New Hampshire 03824, United States. [§] Current address: Physical Chemistry and Applied Spectroscopy, Los Alamos National Laboratory, Los Alamos, New Mexico 87545

ABSTRACT Defining pathways to assemble long-range-ordered 2D nanostructures of specifically designed organic molecules is required in order to optimize the performance of organic thin-film electronic devices. We report on the rapid fabrication of a nearly perfect self-assembled monolayer (SAM) composed of a single-domain 6,13-dichloropentacene (DCP) brick-wall pattern on Au(788). Scanning tunneling microscopy (STM) results show the well-ordered DCP SAM extends over hundreds of nanometers. Combining STM results with insights from density functional theory, we propose that a combination of unique intermolecular and molecule-step interactions drives the DCP SAM formation.

KEYWORDS: self-assembly · pentacene · vicinal single crystal surfaces · gold · scanning tunneling microscopy · polycyclic aromatic hydrocarbons

Organic molecular self-assembly is a bottom-up approach to create molecular architectures that are suitable for a variety of applications including functional materials and molecular electronics.[1−3] Specifically, the ordered assembly of aromatic molecules on crystal substrates for organic electronic applications, such as organic field effect transistor and organic photovoltaic (OPV) devices, has promising technological potential.[4,5] Self-assembled monolayer (SAM) formations are governed by hierarchical interactions including molecule−molecule and molecule−substrate interactions.[6,7] Several strategies and mechanisms for engineering molecular self-assembled architectures on crystal surfaces have been recently reviewed by Barth *et al.*[8,9]

Pentacene, a well-known aromatic compound composed of five linearly arranged benzene rings, is of significant interest for structural and electronic investigations due to its applications in organic electronics.[10,11] While pentacene-based thin-film transistor, OPV, and organic light-emitting diode devices have all been prepared, little is known concerning the effect of molecular orientations and thin-film morphologies on device performance. Before such studies can be undertaken, methods to assemble pentacene and its derivatives into highly ordered, well-defined architectures must be developed. Scanning probe microscopy methods are particularly useful for studying molecular and thin-film architectures. Pentacene's electronic structure has been studied by scanning tunneling microscopy (STM),[12,13] while its chemical bond structure was recently interrogated using high-resolution atomic force microscopy.[14] STM studies on pentacene SAMs on metallic surfaces such as Au(111),[15−17] Au(110),[18] Ag(111),[19−21] Cu(110),[22−24] and Cu(119)[25−27] show in each case, however, that multiple domains form, resulting in superstructures with limited long-range order.

Where device fabrication is concerned, pentacene has several drawbacks including a lack of solubility and poor air stability. Limited solubility hinders device fabrication using high-rate, low-cost methods like spray or blade coating. Facile oxidation of pentacene ultimately degrades device performance and leads to products with limited shelf life. Pentacene derivatives with improved solubility and air stability are currently under study.[28] Several such derivatives including 6,13-dichloropentacene (DCP) show excellent resistance to photo-oxidation and have adjustable HOMO (highest occupied molecular orbital)−LUMO (lowest unoccupied molecular orbital) gaps.[28] The calculated HOMO−LUMO gap of DCP is 2.16 eV compared to 2.29 eV for ordinary pentacene.[28] In general, a gap reduction increases the absorption efficiency of the solar spectrum in OPV applications.[3]

* Address correspondence to jun.wang@unh.edu.

Received for review September 20, 2010 and accepted January 18, 2011.

Published online February 14, 2011
10.1021/nn102468p

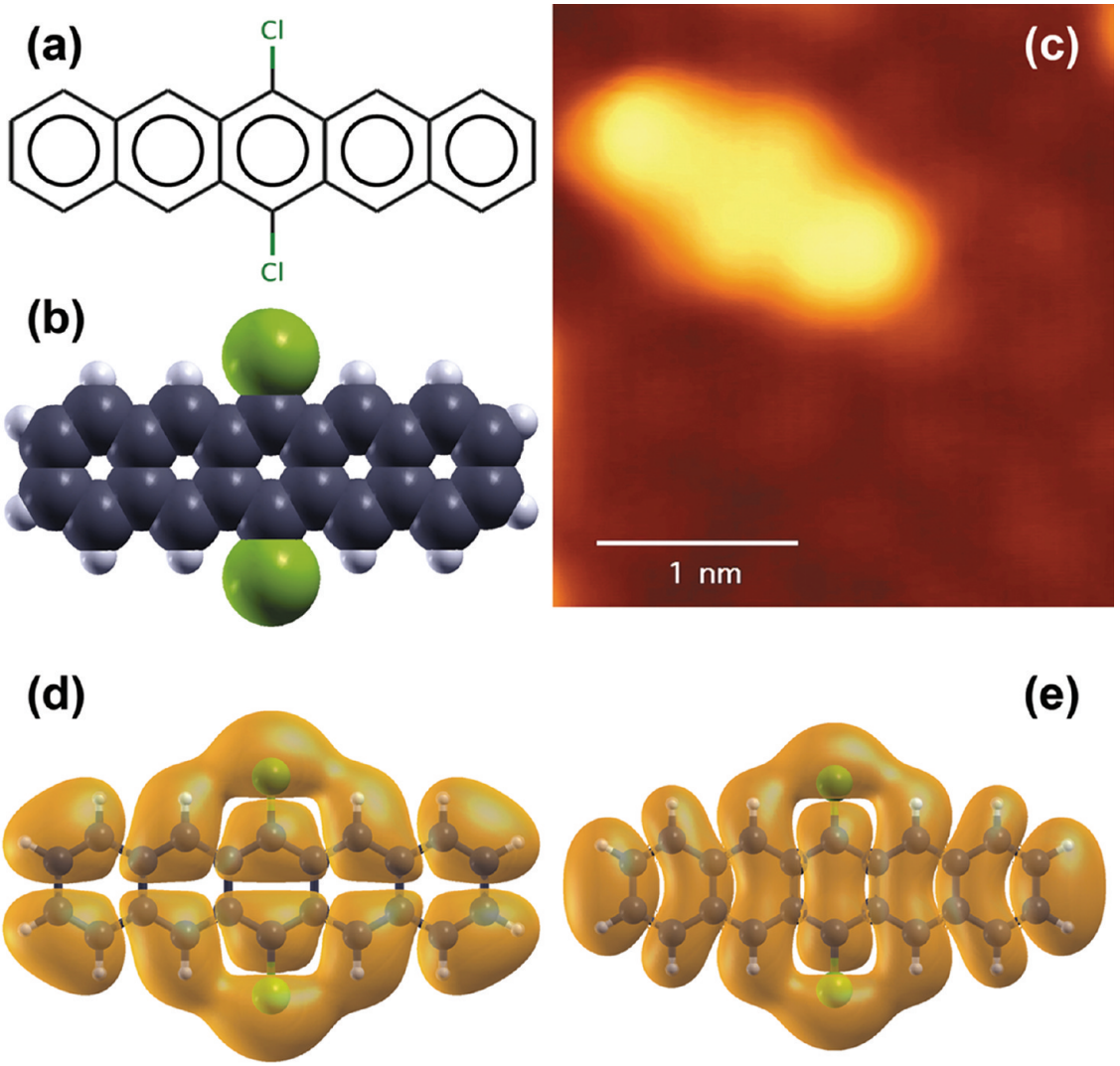

Figure 1. (a) 6,13-Dichloropentacene (DCP) molecular structure. (b) DCP molecular space-filling model: carbon atoms are shown in gray, hydrogen atoms in white, and chlorine atoms in green. (c) High-resolution constant current STM topography of a single spindle-shaped DCP molecule on an atomically resolved gold substrate (295 K, $U_{sample} = +1.3$ V, 0.1 nA). Here, the long axis of the DCP backbone is aligned with the top of three gold atoms along the least compact direction of Au(111). Density functional theory (DFT) simulation of the HOMO (d) and the LUMO (e) for an isolated DCP molecule.

Meanwhile, noble metal vicinal surfaces with tailorable miscut angles and step sizes have been identified as promising templates for molecular self-assembly.[29−32] Au(788), one of the Au(111) vicinal surfaces, is miscut by 3.5° with respect to the (111) orientation toward the [$\bar{2}$11] azimuthal direction, resulting in an one-dimensional array of parallel monatomic steps, each 3.9 nm wide.[29,30] Au(788) has been used as a template for various organic molecular growths, such as C_{60} and PTCDA.[33,34]

Here, we demonstrate the rapid self-assembly of DCP on flat Au(111) terraces and on stepped Au(788) vicinal surfaces. Flat Au(111) terraces support ordered SAM domains with six orientations, while a single-domain SAM with striking long-range order forms on Au(788). These SAM formations are attributed to a delicate energy balance between molecule−molecule interactions and molecule−substrate interactions.[35] Density functional theory (DFT) calculations reveal single-molecule electronic structures and the lattice parameters of a free-standing DCP monolayer. Overall, a comprehensive understanding of the DCP molecular/electronic structures and single-domain SAM formation over large areas is achieved. The results have significant implications for the rapid, low-cost fabrication of organic thin-film electronic devices with precisely defined molecular assemblies.

RESULTS AND DISCUSSION

The DCP molecular structure is shown in Figure 1a, and a space-filling model of DCP molecules with calculated atomic positions is given in Figure 1b. Figure 1c shows a constant current STM topography of a single DCP molecule adsorbed on a flat Au(111)

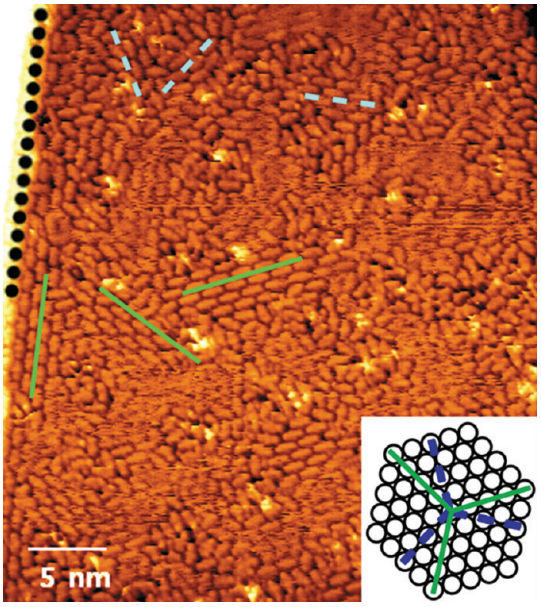

Figure 2. STM image of DCP SAM on a flat Au(111) terrace (295 K, + 0.9 V, 0.1 nA). Ordered domains with six different orientations are distinguished in two groups as marked with green solid and blue dashed lines, respectively. The inset shows those lines moved to a common center. Three green solid (blue dashed) lines, approximately 120° apart, align along the most (least) compact direction of the (111) substrate. The black dotted line denotes one of the compact directions along the step edge of the (111) terrace.

terrace. The brighter spindle-shaped contrast shows the DCP electron orbital contour. The subtle corrugation of the background reveals the atomically resolved gold surface. The long axis of the individual DCP backbone is found to align on top of gold atoms along both, the least or most compact directions of the gold substrate. By comparing Figure 1c with our DFT-calculated HOMO and LUMO electron orbitals of an isolated DCP molecule, shown in Figure 1d,e, respectively, we can infer that the electron orbital contour in the STM topography closely resembles the LUMO structure. This conclusion is also consistent with the tunneling conditions: positive sample bias (+1.3 V) is applied such that electrons tunnel from the tip to the unoccupied electron orbitals of DCP. The tunneling voltage is very similar to the one used to obtain the LUMO topography for pentacene on Au(111).[13]

The DCP molecules start to aggregate with increasing coverage, and ordered structures form close to monolayer coverage on flat Au(111) terraces. Figure 2 shows the DCP SAM on a flat Au(111) terrace with several small, ordered domains of various high-symmetry orientations. We observe six distinct domain orientations sorted in two distinguishable groups, as marked with green solid and blue dashed lines, respectively. Three domain orientations in each group are approximately 120° apart; each domain orientation in one group is perpendicular to a corresponding domain orientation in the other group (Figure 2 inset). These domain orientations suggest that the DCPs align along two preferential orientations with respect to the substrate: the most and the least compact directions (Figure 2 inset). The orientations along the most compact direction are favored, as observed in Figure 2, suggesting a stronger coupling between the molecular orbitals and the surface.

Ordered domains of DCPs on the flat Au(111) terraces are multidirectional and short-ranged. Remarkably, however, a unidirectional, long-range-ordered and stable DCP SAM structure is observed on the vicinal Au(788) surface shown in Figure 3a. Figure 3b shows a perfect long-range-ordered, single-domain DCP SAM on Au(788) with molecular resolution. DCP molecules precisely align in a head-to-tail fashion parallel to the steps, along a most compact direction of the narrow Au(111) terrace. Each step terrace holds exactly five molecular chains. The parallel monatomic steps on Au(788) select only one of the six possible SAM orientations due to the molecule-step interaction. The SAM structure depends closely on the substrate morphology; extra molecules are needed to reside on the kink area of the third step from the left in Figure 3b. The long-range-ordered SAM extends over hundreds of nanometers on well-defined Au(788) steps (Figure 3c).

This DCP SAM structure differs significantly from previously reported pentacene SAM structures on metal surfaces.[15−27] Because of the existence of 6,13 chlorine atoms, each molecule is centered between two molecules of the adjacent rows on both sides. In other words, one molecular row is shifted a half-molecular length with respect to its neighboring row. The resulting superstructure is of significant interest as it resembles a perfect brick-wall pattern. For pure pentacene, no such row-by-row half-molecular-length-shifted superstructure is known to exist. With 6,13 chlorines in place, DCP has less freedom along the backbone long-axis direction. The calculated closest contact Cl−H distance between atoms from two adjacent molecules is 0.277 nm, with the C−H−Cl angle of 142° (Figure 3d); the calculated closest H−H distance between two DCP molecules in neighboring rows is 0.207 nm, and within the same row, it is 0.213 nm. These H−H van der Waals interactions should be weaker in strength than the Cl−H hydrogen-bonding interaction, suggesting that intermolecular hydrogen bonding plays an important role in SAM formation and long-range order.

In addition, we find that, even on some narrower steps on the same surface, DCPs still arrange themselves in the unidirectional, long-range-ordered fashion (Figure 4). The narrower steps of approximately 1.6 nm width are believed to represent a (577) surface region, belonging to the family of {111} step vicinal surfaces.[30] The molecular brick wall is preserved along the step, and each narrow terrace holds only two molecular chains (Figure 4) forming a ribbon structure.

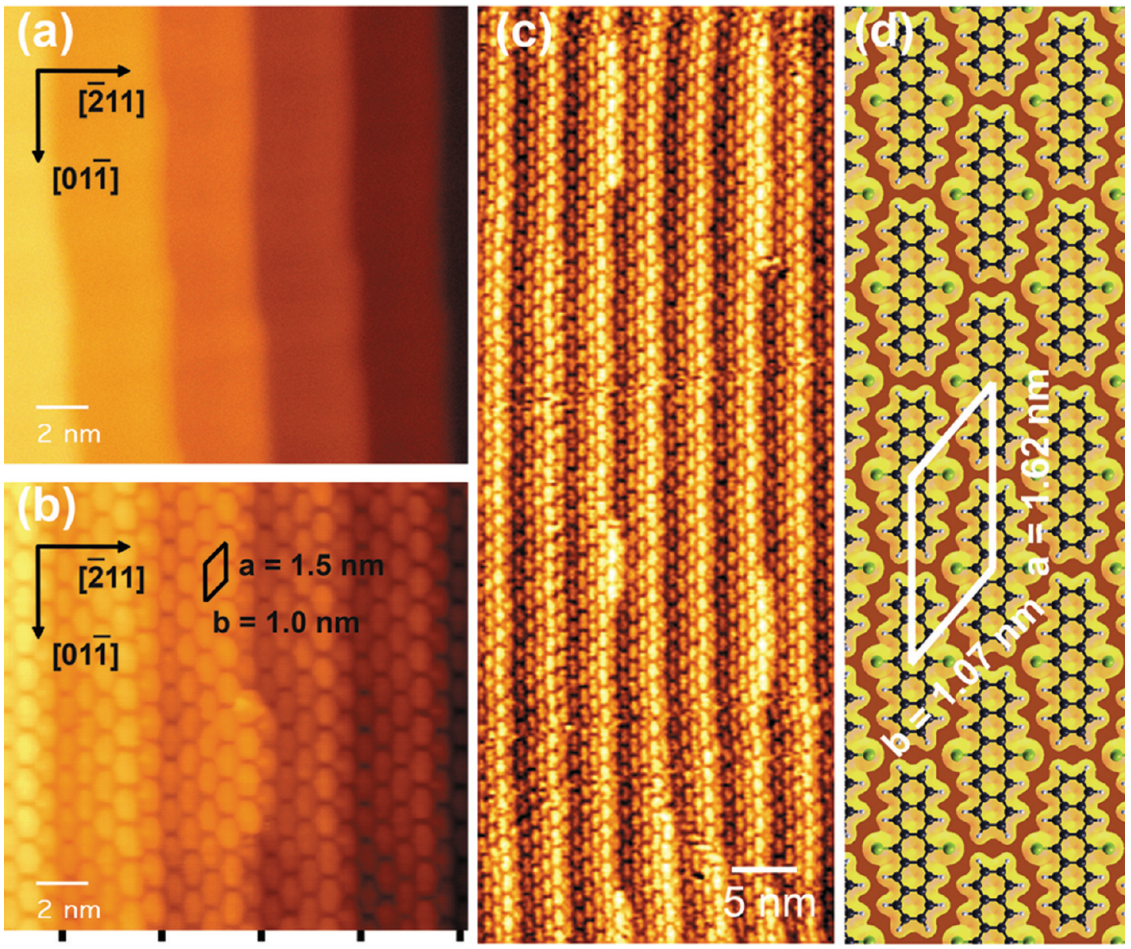

Figure 3. (a) Clean-stepped Au(788) vicinal surface. (b) DCP SAM on Au(788) (295 K, + 0.9 V, 0.1 nA); each step holds five rows of close-packed DCP with an oblique unit cell of approximately 1.5 nm × 1 nm. The substrate orientation is the same as in (a). The black dashes on the bottom indicate the step edge locations. (c) Large-scale (slope-corrected) STM image of highly long-range-ordered DCP SAM on Au(788) (295 K, + 0.9 V, 0.1 nA). (d) DFT model of the free-standing DCP SAM structure. Each row is shifted by a half-molecular length with respect to its adjacent row to form a molecular brick-wall structure. The calculated value of the unit cell is 1.62 nm × 1.07 nm.

Overall, the SAM structures are consistent on both flat and stepped vicinal surfaces. The unit cell of the ordered SAM is approximately 1.5(±0.1) nm × 1.0(±0.1) nm, with an acute angle of approximately 42°. This is consistent with DFT calculated results for the free-standing DCP monolayer (Figure 3d) that give a unit cell of 1.62 nm × 1.07 nm with a 40.5° angle. All findings lead to the conclusion that center-shifted molecular rows (*i.e.*, brick-wall SAMs) represent the best possible option for minimizing intermolecular hydrogen-bonding energies while maintaining favorable molecule-step interactions. While the DCP brick-wall SAM can form regardless of the stepped surface, the stepped surface forces the molecules to assemble into one direction with extraordinary long-range order. Furthermore, the step width controls the number of molecular chains on each terrace.

CONCLUSION

We have demonstrated the rapid fabrication of a nearly perfect self-assembled monolayer (SAM) composed of single-domain 6,13-dichloropentacene (DCP) over large areas on Au(788). The DCP molecules precisely organize into a center-shifted brick-wall structure on the stepped Au(788) surface. Scanning tunneling microscopy results show that the ordered DCP SAM extends over hundreds of nanometers. These findings strongly suggest that a bottom-up strategy of molecular self-assembly is a feasible approach for the rapid fabrication of organic molecular electronic devices with precisely controlled thin-film architectures.

METHODS

Our experiments were performed in an ultrahigh vacuum chamber with a base pressure of ≤1.0 × 10^{-10} mbar. The Au(788) vicinal single crystal surface was cleaned by repeated cycles of argon ion sputtering (600 eV, 1.0 × 10^{-5} mbar), followed by annealing up to 500 °C. The DCP molecules, in

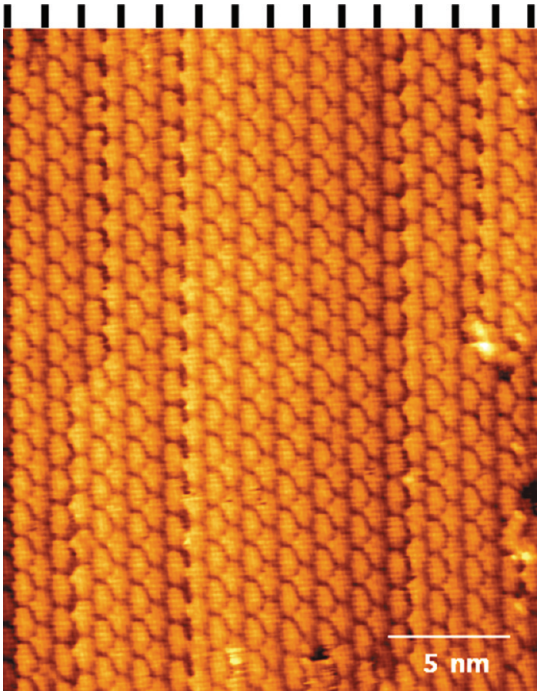

Figure 4. STM image of DCP SAM on narrower, 1.6 nm wide, gold steps (295 K, +0.9 V, 0.1 nA). The black dashes on the top indicate the step edge locations. Each narrow terrace holds two molecular chains forming a ribbon structure.

powder form, were deposited *in situ* onto the surface at room temperature *via* physical vapor deposition from a home-built Knudsen cell, and the molecular coverage was controlled by exposure time. The flux used throughout our study was approximately 6 ML/h or 10 min per single DCP monolayer. The STM images were acquired by a SPECS-Aarhus system at room temperature. Our DFT calculations were carried out using the ABINIT package employing a plane-wave basis set for a repeated-slab structure.[36] We used the local density approximation (LDA) with Troullier−Martins pseudopotentials. The Brillouin zone integrations for the DCP lattice used a 4 × 3 k-point grid. The vacuum gap between the slabs was fixed at 1.06 nm. The plane-wave cutoff energy was set to 50 hartree. The atomic positions and in-plane lattice constants were relaxed until the forces were less than 0.025 eV/nm under the constraint of one molecule per unit cell.

Acknowledgment. This work is supported by the NSF-funded Nanoscale Science and Engineering Center for High-rate Nanomanufacturing (NSF EEC-0425826), the NSF-funded New Hampshire Experimental Program to Stimulate Competitive Research (NSF EPS-0701730), and NSF DMR-1006863.

REFERENCES AND NOTES

1. Service, R. F. Can Chemists Assemble a Future for Molecular Electronics? *Science* **2002,** *295*, 2398–2399.
2. Joachim, C.; Gimzewski, J. K.; Aviram, A. Electronics Using Hybrid-Molecular and Mono-Molecular Devices. *Nature* **2000,** *408*, 541–548.
3. Peet, J.; Heeger, A. J.; Bazan, G. C. "Plastic" Solar Cells: Self-Assembly of Bulk Heterojunction Nanomaterials by Spontaneous Phase Separation. *Acc. Chem. Res.* **2009,** *42*, 1700–1708.
4. Witte, G.; Woll, C. Growth of Aromatic Molecules on Solid Substrates for Applications in Organic Electronics. *J. Mater. Res.* **2004,** *19*, 1889–1916.
5. Hoppe, H.; Sariciftci, N. S. Organic Solar Cells: An Overview. *J. Mater. Res.* **2004,** *19*, 1924–1945.
6. Sykes, E. C. H.; Han, P.; Kandel, S. A.; Kelly, K. F.; McCarty, G. S.; Weiss, P. S. Substrate-Mediated Interactions and Intermolecular Forces between Molecules Adsorbed on Surfaces. *Acc. Chem. Res.* **2003,** *36*, 945–953.
7. Diaconescu, B.; Yang, T.; Berber, S.; Jazdzyk, M.; Miller, G. P.; Tománek, D.; Pohl, K Molecular Self-Assembly of Functionalized Fullerenes on a Metal Surface. *Phys. Rev. Lett.* **2009,** *102*, 056102.
8. Barth, J. V.; Costantini, G.; Kern, K. Engineering Atomic and Molecular Nanostructures at Surfaces. *Nature* **2005,** *437*, 671–679.
9. Barth, J. V. Molecular Architectonic on Metal Surfaces. *Annu. Rev. Phys. Chem.* **2007,** *58*, 375–407.
10. Heringdorf, F. J. M. Z.; Reuter, M. C.; Tromp, R. M. Growth Dynamics of Pentacene Thin Films. *Nature* **2001,** *412*, 517–520.
11. Bredas, J. L.; Norton, J. E.; Cornil, J.; Coropceanu, V. Molecular Understanding of Organic Solar Cells: The Challenges. *Acc. Chem. Res.* **2009,** *42*, 1691–1699.
12. Repp, J.; Meyer, G.; Stojkovic, S. M.; Gourdon, A.; Joachim, C. Molecules on Insulating Films: Scanning-Tunneling Microscopy Imaging of Individual Molecular Orbitals. *Phys. Rev. Lett.* **2005,** *94*, 026803.
13. Soe, W. H.; Manzano, C.; De Sarkar, A.; Chandrasekhar, N.; Joachim, C. Direct Observation of Molecular Orbitals of Pentacene Physisorbed on Au(111) by Scanning Tunneling Microscope. *Phys. Rev. Lett.* **2009,** *102*, 176102.
14. Gross, L.; Mohn, F.; Moll, N.; Liljeroth, P.; Meyer, G. The Chemical Structure of a Molecule Resolved by Atomic Force Microscopy. *Science* **2009,** *325*, 1110–1114.
15. France, C. B.; Schroeder, P. G.; Forsythe, J. C.; Parkinson, B. A. Scanning Tunneling Microscopy Study of the Coverage-Dependent Structures of Pentacene on Au(111). *Langmuir* **2003,** *19*, 1274–1281.
16. Kang, J. H.; Zhu, X. Y. Layer-by-Layer Growth of Incommensurate, Polycrystalline, Lying down Pentacene Thin Films on Au(111). *Chem. Mater.* **2006,** *18*, 1318–1323.
17. Pong, I.; Yau, S.; Huang, P. Y.; Chen, M. C.; Hu, T. S.; Yang, Y. C.; Lee, Y. L. *In Situ* STM Imaging of the Structures of Pentacene Molecules Adsorbed on Au(111). *Langmuir* **2009,** *25*, 9887–9893.
18. Guaino, P.; Carty, D.; Hughes, G.; McDonald, O.; Cafolla, A. A. Long-Range Order in a Multilayer Organic Film Templated by a Molecular-Induced Surface Reconstruction: Pentacene on Au(110). *Appl. Phys. Lett.* **2004,** *85*, 2777–2779.
19. Eremtchenko, M.; Temirov, R.; Bauer, D.; Schaefer, J. A.; Tautz, F. S. Formation of Molecular Order on a Disordered Interface Layer: Pentacene/Ag(111). *Phys. Rev. B* **2005,** *72*, 115430.
20. Dougherty, D. B.; Jin, W.; Cullen, W. G.; Reutt-Robey, J. E.; Robey, S. W. Variable Temperature Scanning Tunneling-Microscopy of PentaceneMonolayer and Bilayer Phases on Ag(111). *J. Phys. Chem. C* **2008,** *112*, 20334–20339.
21. Wong, S. L.; Huang, H.; Huang, Y. L.; Wang, Y. Z.; Gao, X. Y.; Suzuki, T.; Chen, W.; Wee, A. T. S. Effect of Fluorination on the Molecular Packing of Perfluoropentacene and Pentacene Ultrathin Films on Ag(111). *J. Phys. Chem. C* **2010,** *114*, 9356–9361.
22. Lukas, S.; Witte, G.; Woll, C. Novel Mechanism for Molecular Self-Assembly on Metal Substrates: Unidirectional Rows of Pentacene on Cu(110) Produced by a Substrate-Mediated Repulsion. *Phys. Rev. Lett.* **2002,** *88*, 028301.
23. Chen, Q.; McDowall, A. J.; Richardson, N. V. Ordered Structures of Tetracene and Pentacene on Cu(110) Surfaces. *Langmuir* **2003,** *19*, 10164–10171.
24. Martinez-Blanco, J.; Ruiz-Oses, M.; Joco, V.; Sayago, D. I.; Segovia, P.; Michel, E. G. Ordered Structures of Pentacene on Cu(110). *J. Vac. Sci. Technol., B* **2009,** *27*, 863–867.
25. Gavioli, L.; Fanetti, M.; Sancrotti, M.; Betti, M. G. Long-Range-Ordered Pentacene Chains Assembled on the Cu(119) Vicinal Surface. *Phys. Rev. B* **2005,** *72*, 035458.
26. Fanetti, M.; Gavioli, L.; Sancrotti, M. Long-Range-Ordered, Molecular-Induced Nanofaceting. *Adv. Mater.* **2006,** *18*, 2863–2867.
27. Annese, E.; Viol, C. E.; Zhou, B.; Fujii, J.; Vobornik, I.; Baldacchini, C.; Betti, M. G.; Rossi, G. Self Organization of

Pentacene Grown on Cu(119). *Surf. Sci.* **2007,** *601*, 4242–4245.
28. Kaur, I.; Jia, W. L.; Kopreski, R. P.; Selvarasah, S.; Dokmeci, M. R.; Pramanik, C.; Mc-Gruer, N. E.; Miller, G. P. Substituent Effects in Pentacenes: Gaining Control over HOMO–LUMO Gaps and Photooxidative Resistances. *J. Am. Chem. Soc.* **2008,** *130*, 16274–16286.
29. Repain, V.; Baudot, G.; Ellmer, H.; Rousset, S. Two-Dimensional Long-Range-Ordered Growth of Uniform Cobalt Nanostructures on a Au(111) Vicinal Template. *Europhys. Lett.* **2002,** *58*, 730–736.
30. Rousset, S.; Repain, V.; Baudot, G.; Garreau, Y.; Lecoeur, J. Self-Ordering of Au(111) Vicinal Surfaces and Application to Nanostructure Organized Growth. *J. Phys.: Condens. Matter* **2003,** *15*, S3363–S3392.
31. Kuhnke, K.; Kern, K. Vicinal Metal Surfaces as Nanotemplates for the Growth of Low-Dimensional Structures *J. Phys.: Condens. Matter* **2003,** *15*, S3311–S3335.
32. Zaki, N.; Potapenko, D.; Johnson, P. D.; Osgood, R. M. Atom-Wide Co Wires on Cu(775) at Room Temperature. *Phys. Rev. B* **2009,** *80*, 155419.
33. Neel, N.; Kroger, J.; Berndt, R. Highly Periodic Fullerene Nanomesh. *Adv. Mater.* **2006,** *18*, 174–177.
34. Kroger, J.; Neel, N.; Jensen, H.; Berndt, R.; Rurali, R.; Lorente, N. Molecules on Vicinal Au Surfaces Studied by Scanning Tunnelling Microscopy. *J. Phys.: Condens. Matter* **2006,** *18*, S51–S66.
35. Nenchev, G.; Diaconescu, B.; Hagelberg, F.; Pohl, K. Self-Assembly of Methanethiol on the Reconstructed Au(111) Surface. *Phys. Rev. B* **2009,** *80*, 081401(R).
36. Gonze, X.; Amadon, B.; Anglade, P. M.; Beuken, J. M.; Bottin, F.; Boulanger, P.; Bruneval, F.; Caliste, D.; Caracas, R.; Cote, M.; *et al.* ABINIT: First-Principles Approach to Material and Nanosystem Properties. *Comput. Phys. Commun.* **2009,** *180*, 2582–2615.